Title

Three-dimensional morphological variability of Recent rhynchonellide brachiopod crura

Journal

Paleobiology, 40(4)

ISSN

0094-8373

Authors

Schreiber, Holly A
Roopnarine, Peter D
Carlson, Sandra J

Publication Date

2014

DOI

10.1666/13042

Peer reviewed

Three-dimensional morphological variability of Recent rhynchonellide brachiopod crura

Holly A. Schreiber, Peter D. Roopnarine, and Sandra J. Carlson

Abstract.—

Crura, the calcareous support structures of the lophophore in rhynchonellide brachiopods, have historically been used to justify higher-level rhynchonellide classification and reveal major evolutionary lineages within rhynchonellides. Seventeen crural types have been described and categorized into four groups based on variation in overall structure and cross-sectional shape, but not evaluated in a quantitative or comprehensive manner. Heterochrony has been hypothesized to play a role in the evolutionary transitions among some types, but the structural, developmental, and phylogenetic context for testing these hypotheses has not yet been established. In this study, we quantify morphological disparity among all six crural morphs in Recent adult rhynchonellides using three-dimensional geometric morphometric techniques, with the goal of delineating more objective criteria for identifying and comparing crural morphs, ultimately to test hypotheses explaining morphological transformations in ontogeny and phylogeny. We imaged the crura of seven Recent rhynchonellide species using X-ray computed microtomography. We used landmarks and semi-landmarks to define the dimensions and curvature of the crura and the surrounding hinge area. Procrustes-standardized landmark coordinates were analyzed using a principal component analysis to test the discreteness of the individual crural morphs, groups of morphs, and identify features that vary most among the crural configurations.

Our results demonstrate that microCT imaging techniques provide novel ways to investigate the morphology of very small features that may be otherwise impossible to obtain using more conventional imaging techniques. Although we predicted overlap among crural morphs in the 3D shape space, the principal component analyses suggest that five of the six crural morphs differ distinctly from one another. Some but not all previously designated crural groups appear to

exhibit morphological cohesion. This study establishes a quantitative morphological foundation necessary to begin an investigation of the phylogenetic significance of ontogenetic changes in crura, which will allow hypotheses of heterochrony to be tested.

Holly A. Schreiber and Sandra J. Carlson. Department of Earth and Planetary Sciences, University of California, Davis, One Shields Avenue, Davis, California 95616 U.S.A. E-mail: haschultz@ucdavis.edu; sjcarlson@ucdavis.edu.

Peter D. Roopnarine. Department of Invertebrate Zoology and Geology, California Academy of Sciences, 55 Music Concourse Drive, San Francisco, California 94118 U.S.A. E-mail: proopnarine@calacademy.org.

Introduction

Crura, the prong-like, calcareous structures that support the lophophore on either side of the mouth, are often the most conspicuous morphological features of the interior of rhynchonellide brachiopod dorsal valves (Fig. 1). The crura support and position the base of the lophophore, allowing the lophophore to filter water efficiently as it enters the mantle cavity along either side of the commissure and exits at the valve anterior (Ager 1965; Rudwick 1970; Williams et al. 1997). A broad range of crural morphological variability exists — 17 named types — even though all rhynchonellides are characterized by only one lophophore type, the helically-coiled spirolophe lophophore (Rudwick 1970; Williams et al. 1997; Savage et al. 2002). The morphological diversity among crura has historically been used to organize higher-level rhynchonellide classification (Manceñido 1998, 2000; Manceñido and Owens 2001; Savage et al.

2002; Manceñido et al. 2007), but it remains unclear how different named crural configurations are related morphologically, phylogenetically, or ontogenetically (Cooper 1959; Ager 1965; Rudwick 1970; Manceñido and Owens 2001; Savage et al. 2002; Manceñido 1998, 2000; Manceñido et al. 2007; Manceñido and Motchurova-Dekova 2010). A quantitative characterization of crural morphology would facilitate reproducibility in the naming of crural types (morphs) and in the identification of specimens with respect to crural type, and allow us to test proposed evolutionary patterns of crural transformation (Manceñido and Motchurova-Dekova 2010). It would also enable quantitative comparisons among adults, throughout ontogeny, and across phylogenetic hypotheses of relationship (Cohen and Bitner 2013; Schreiber et al. 2013). Using microCT technology, we obtained 3D images of all six named crural types expressed in Recent rhynchonellides, and statistically analyzed three-dimensional geometric morphometric measurements of crura in order to evaluate the relationship between size and shape of crura in rhynchonellides of different body (shell) size, taxonomic affiliation, and phylogenetic affinity.

Crura in Rhynchonellida

Rhynchonellida originated in the Ordovician and is the second most diverse extant brachiopod order (after Terebratulida), with over 500 fossil and extant genera (Williams et al. 2000a, 2000b; Carlson and Leighton 2001; Savage et al. 2002; Manceñido et al. 2007). Today, forty extant species are classified into nineteen genera. They are distributed globally, but are most abundant and diverse in extra-tropical regions, specifically Australia and New Zealand (Savage et al. 2002; Logan 2007; Savage 2007; Manceñido et al. 2007). Although rhynchonellide (Kuhn 1949) brachiopods are the geologically oldest and putatively the phylogenetically most basal of the extant rhynchonelliforms, they are somewhat inconspicuous in today's oceans with

many living in patchy distributions at bathyal depths. Their apparent rarity in modern faunas makes numerous species difficult to collect in abundance and consequently they are relatively understudied by neontologists and paleontologists. Rhynchonellide extant diversity — approximately 3% of their total Phanerozoic generic diversity — is severely diminished, however their apparently basal phylogenetic position provides, among crown clade articulate brachiopods, critically important comparative information about the evolution of more derived rhynchonelliform brachiopods (Cooper 1959; Ager 1965; Carlson 1995; Cohen and Gawthrop 1997; Manceñido and Owens 2001; Cohen 2001a, 2001b, 2007; Carlson and Leighton 2001; Savage et al. 2002; Cohen and Weydmann 2005; Carlson 2007; Manceñido et al. 2007).

Extant rhynchonellides have a spirolophe lophophore (with the exception of *Tethyrhynchia*, which is trocholophous) in which the apices of the spires point dorsally, and are supported posteriorly by crura (Williams et al. 1997; Savage 1996; Manceñido and Owen 2001; Savage et al. 2002). Their distinctive, roughly triangular shell morphology is often characterized by a strongly biconvex and costate shell in extinct forms, usually with a dorsal fold and ventral sulcus (though many today are rectimarginate and lack shell ornamentation). Extant adult rhynchonellides range in shell length from approximately one millimeter (e.g., *Tethyrhynchia mediterranea*) to twenty millimeters (e.g., *Pemphixina pyxidata*); compared to terebratulides, they are relatively small as adults.

Crura (singular: crus) are short (typically no more than one or two millimeters long), paired, rod- or prong-like calcareous processes (Fig. 1). Crura extend antero-ventrally from the inner socket ridge of the dorsal valve into the mantle cavity on either side of the mouth of the brachiopod, from which the lophophore arms extend, and serve as attachment sites for the body wall (Rudwick 1970; Brunton et al. 1996; Williams et al. 1997; Savage et al. 2002). Each crus

supports the very proximal section of the lophophore directly adjacent to the mouth, while the remaining portion of the spirolophe is supported hydrostatically, lacking any additional mineralized support (Rudwick 1970; James et al. 1992). Due to their typically short length, the crura act primarily as positioning devices for the lophophore rather than extensive support structures, and consequently, their geometry may affect the three-dimensional flow of water through the mantle cavity (Ager 1965; Rudwick 1970; Williams et al. 1997). However, the specific details of the relationship between crural morphology, and lophophore geometry and water flow patterns, have yet to be studied (although see LaBarbera 1977, 1978, 1981; Emig 1992; Shiino et al. 2009; Shiino and Kuwazuru 2010). Crura vary morphologically in three primary ways: angle of projection into the mantle cavity, toward the ventral valve shell (curvature of the crus); shape of the distal tip of the crus (narrow or broad, digitate or not); and cross-sectional shape of the crus (straight or curved, and curved dorsally/ventrally). Crural morphs range from laterally to dorso-ventrally compressed and can either be relatively straight or highly curved or twisted medially in a gentle helix (Fig. 2).

The crura begin to develop in juvenile rhynchonellides shortly after larval settlement (Long and Stricker 1991; James et al. 1992; Williams et al. 1997). Sheathed in outer epithelium, they consist of secondary shell material (Rudwick 1970; Williams et al. 1997) and develop from the inner socket ridge, growing by simple accretion to the distal end. Rudwick (1970) claims that crura grow through ontogeny without resorption of shell material, but this is a hypothesis that has yet to be tested. The tips of the crura may be elongated into the primary lamellae of spire-bearing brachiopods (e.g., extinct atrypides, athyridides, and spiriferides) or the descending lamellae of loops in terebratulide brachiopods (Williams et al. 1997); all are groups that have evolved from within a paraphyletic Rhynchonellida or share close common ancestry with them (Carlson 2007).

Crura are thus an important component of the cardinalia of all crown clade articulated brachiopods (Neoarticulata; Carlson 2012; Carlson and Cohen, in press).

Over the past 150 years, seventeen crural configurations have been named and have recently been placed into four qualitative groups (raducal, septifal, ensimergal, arcual) according to differences in overall structure and cross-sectional shape (Fig. 2; Manceñido 1998, 2000; Savage et al. 2002; Manceñido et al. 2007; Manceñido and Motchurova-Dekova 2010). The depauperate Recent rhynchonellide fauna represents not only a small fraction of taxonomic diversity, but also a fraction of the morphological diversity of crura found in the geologic past (Manceñido and Owens 2001; Savage et al. 2002). Under the current classification, nine rhynchonellide superfamilies have the same crural type, while six superfamilies are characterized by multiple crural types including the four superfamilies with extant representatives (Cooper 1959; Ager 1965; Carlson and Leighton 2001; Manceñido and Owens 2001; Savage et al. 2002).

Do adult individuals within a single morph vary significantly in shape, or exhibit similar degrees of variability from morph to morph? After surveying rhynchonellide crural variation present in museum collections and literature sources (see complete list in Supplementary Table 1), we noted that slight qualitative shape variations in the crura, often found in only a few specimens, were used as the basis for naming new crural morphs; a fact that Cooper (1959) and Ager (1965) and others confirmed in their descriptions. A thorough comparative review of rhynchonellide crural morphs is called for because no consistent method has been used historically to identify, name, or group them, or to determine relationships among morphs or among groups of morphs. Arguably, the best way to achieve this revision is to use both qualitative and quantitative methods, as each can illuminate the other. Qualitative descriptions of individual crural morphs exist (see Rothpletz 1886; Wisniewska 1932; Cooper 1959; Ager 1962,

1965; Dagys 1968; Rudwick 1970; Baranov 1980; Savage et al. 2002; Manceñido and Motchurova-Dekova 2010) and include brief discussions of crural shape variability. However, these descriptions can vary from author to author depending on the particular specimens studied, revealing the need for quantitative analyses that can test hypotheses using measurable data in a more objective and repeatable manner.

Our study is the first to undertake a quantitative analysis of crura in an effort to identify and classify the range of variability present in extant rhynchonellides. We have chosen to characterize Recent crural morphs using computer generated three-dimensional surface models, which allow in-depth examination of very small crural features not easily seen with more conventional imaging and analytical methods. The three-dimensional surface models can be enlarged and manipulated fully in three dimensions to reveal multiple views of the crura from many perspectives (Fig. 3). We then use three-dimensional geometric morphometric and multivariate statistical analyses to quantify the morphological diversity within and among the six crural morphs present in Recent rhynchonellides. How distinct are each of these six morphs from one another and how are they related in size and shape? How does the raduliform morph, the stratigraphically oldest and most common crural (Savage et al. 2002) form vary among adults? Because several different names have been given to the morphologically simple crura lacking quantitative analysis, we predict that crural morphs have been over-split and may occupy overlapping regions in three-dimensional shape space.

Materials and Methods

We selected extant rhynchonellide species for this initial morphometric study because crura can be imaged more precisely in three-dimensions using X-ray computed microtomography when the mantle cavity is entirely free of sediment. By using only Recent

specimens, we also avoid complications from post-mortem distortion of the crura, a confounding problem that will be examined in future studies. A minimum of three individuals of each of the six extant crural morphs (raduliform, falciform, arcuiform, canaliform, spinuliform, maniculiform; Fig. 3), from seven species, were selected from museum and marine laboratory collections, for a total of twenty-three adult rhynchonellides (see Supplementary Table 1 for a complete list). Specimens were examined from the National Museum of Natural History (Smithsonian Institution, Washington, D. C.), the California Academy of Sciences (San Francisco, CA), Portobello Marine Laboratory (Portobello, New Zealand), University of California, Davis, and Scripps Institution of Oceanography (San Diego, CA), and were either dried or preserved in 70% ethanol.

Images of the crura were obtained using X-ray computed microtomography (microCT). Using X-rays, microCT scanners generate a series of digital, contiguous two-dimensional cross-sectional slices of an object by detecting differences in the attenuation of the X-rays as they pass through the object. Materials will scatter or absorb X-rays in direct relation to their density. A more dense material will appear more opaque in a microCT image than a less dense material (Elliot and Dover 1982; Flannery et al. 1987; Ketcham and Carlson 2001; Monnet et al. 2009; Shiino et al. 2009; Peck et al. 2009; Angiolini et al. 2010; Motchurova-Dekova and Harper 2010; Pakhnevich 2010; van Dam et al. 2011; Abel et al. 2012; Görög et al. 2012). The microCT scanner produces a series of sequential, adjacent two-dimensional images which, when assembled using computer software such as 3D Slicer (http://www.slicer.org; Gering et al. 1999; Pieper et al. 2004; Pieper et al. 2006), create a three-dimensional model of the object (Ketcham and Carlson 2001). These three-dimensional representations can then be easily manipulated digitally, by rotation in three dimensions, for ease of measurement and visualization of features.

We imaged all specimens with the Scanco Medical microCT scanner located at the University of California, Davis School of Veterinary Medicine. The scanner is a desktop cone-beam microCT scanner with a nominal resolution of approximately five to ninety microns. Samples require no preparation and can be scanned either dried or preserved in alcohol. With this initial set of images of extant crura as a baseline, to establish proof of concept, we can then attempt to obtain images of fossil crura, from individuals preserved in sediment matrix of a range of densities. Individual image slices were assembled and surface models constructed using the software platforms Amira v5.2 or 3D Slicer v3.4. The surface models were then edited and enhanced in the program Raindrop GeoMagic Studio v10.0 to expose the crura and other internal features of the shell such as the sockets, hinge plates, and socket ridges (Fig 1).

We used three-dimensional geometric morphometric techniques to quantify the disparity among the six crural morphs found in extant rhynchonellides. Landmarks, along with semi-landmarks, defined the dimensions of the crura, cardinalia, and the curvature of the crura (Fig. 4). A landmark is a discrete, geometrically homologous anatomical point that can be accurately identified on all individuals, while a semi-landmark is a constructed point on a geometric feature, often a curve or surface, defined by its relative position on that feature (Bookstein 1991; Zelditch et al. 2004). We defined nine homologous landmarks (Types 1 and 2; Bookstein 1991). Three-dimensional Cartesian coordinates were collected for all landmarks and semi-landmarks (Mitteroecker and Gunz 2002; Zelditch et al. 2004) using the morphometric program Landmark v3.6 (Wiley et al. 2007).

Crural curvature and the shape of the distal tip are important characteristics for defining crural morphs; therefore we used semi-landmarks to delineate the curved areas of the crus (e.g., distal tip morphology; Bookstein 1997; Gunz 2001, 2005; Gunz et al. 2005; Mitteroecker and

Gunz 2009; see Table 1 for a complete description of all landmarks and semi-landmarks). Semi-landmarks allow information about the curvature of a feature to be incorporated into a geometric morphometric analysis (Zelditch et al. 2004). Each curve consists of three equally spaced semi-landmarks anchored by two landmarks. Bilateral symmetry allowed landmarks to be digitized on one crus per specimen, useful in cases in which one crus was damaged or broken off entirely.

Following data collection, we used the morphometric program Morphologika v2.5 (O'Higgins and Jones 1998), to perform a generalized Procrustes analysis (Gower 1975; Rohlf and Slice 1990), which removed any variation between sets of landmarks due to differences in scale, rotation, or translation. A generalized Procrustes analysis performs a Procrustes superimposition which minimizes the Procrustes distance among all landmark configurations in the dataset using centroid size (Gower 1975; Rohlf and Slice 1990; Zelditch et al. 2004). The Procrustes-fitted coordinates served as input variables for multivariate statistical analyses. We first examined shape distinct from size, and later added size back into the analysis by comparing shape with centroid size of landmark and semi-landmark data.

We used multivariate statistical analyses to explore the nature of morphological variation among crural morphs in order to locate the areas of the crura that vary most among Recent morphs and to test statistically the morphological distinctiveness and examine within-morph variability of the six Recent crural morphs. A principal component analysis (PCA) was used to locate and explore areas of the crura that exhibit the most variability and to study the variation of landmark positions between the Recent crural morphs, allowing shape parameters that vary among crural morphs to be identified. The PCA of the measured variables was completed in the program PAST v1.94b (Hammer et al. 2001) with the variance-covariance matrix of the unstandardized data (i.e., the variance of the data is not standardized), allowing the areas of

maximum shape variation to be identified. We also performed cluster analyses, both single linkage and neighbor-joining, based on the Euclidean distances between specimens, as measured using scores derived from the first three principal components of the PCA, in order to test whether individuals in the same crural type cluster together and whether different types cluster together.

We evaluated morphological variability within and among six crural morphs in adults of seven species (representing four superfamilies) of rhynchonellides, variability among the raduliform crura of adults of two species, and, to a more limited degree, variability within and among the arcual and raducal groups (Manceñido and Motchurova-Dekova 2010). Adult morphological variation of crural morphs was assessed using a PCA of all crura from adult rhynchonellides using a combination of landmark and semi-landmark data. Differences in crural shape have been deemed to be more important than absolute changes in size in naming crural morphs (Savage et al. 2002; Manceñido et al. 2007). Shape and orientation also appear to influence the way in which the crura contact and support the lophophore (Cooper 1959; Manceñido and Owen 2001; Savage et al. 2002; Manceñido et al. 2007). To assess within-morph variability, we performed a PCA on the Procrustes coordinates derived from specimens having raduliform crura (adult *Notosaria nigricans* and *Hemithiris psittacea*). Shape differences found among the crural groups designated by Manceñido and Motchurova-Dekova (2010) were investigated also using a PCA. Qualitative differences among the crural morphs, and the biological implications of those differences, were also evaluated.

Results

Adult Morphological Variation.— The principal component that accounts for the greatest amount of variation in this analysis, PC 1, is associated with landmarks and semi-landmarks that

describe the ventral position of the medial edge of the crus (Fig. 5). The first three PC axes account for 64.83% of the total variance in the data: PC 1 accounts for 27.73%, PC 2 accounts for 25.37%, and PC 3 accounts for 11.73% (complete PC scores are available from the authors for all analyses). The morphological variation illustrated along PC 1 is associated with the width and the medial twist of the distal end of the crus relative to the proximal end (Fig. 5A). Falciform crura represent one morphological extreme with broad, medially convex crura. Arcuiform crura represent the opposite extreme with narrower crura twisted medially. All other crural morphs are concentrated around the origin, indicating that the width and twisting of the distal end of the crura dominate variation along PC 1. The morphological variation illustrated along PC 2 is associated with crus length and width and ventral curvature (Fig. 5A). Maniculiform crura represent one end-member with narrow, straight and elongated crura. They are also the smallest crura in absolute size (Fig. 3). Canaliform represent the opposite end-member morphology with short, wide crura, and are among the largest crura which occur in the largest individuals. Crural morphs are more or less equally distributed along PC 2 indicating slight variations in crural width and length and ventral curvature from one end-member to the other. Morphological variation along PC 3 is associated with crural curvature and medial twisting (Fig. 5B); *Hemithiris* distal tips are horizontal; *Frieleia* are nearly vertical, and only slightly medially tilted. Variation along PC 3 ranges from relatively straight and laterally compressed spinuliform crura to dorso-ventrally compressed, medially twisted, and ventrally curved in raduliform crura. Crural morphs are more or less equally distributed along PC 3 indicating slight variations in crural curvature from one extreme to the other. Semi-landmarks along the medial edge of the crus have a significant impact on the outcome of the analysis by capturing the variability of the medial edge of the crus and subsequently outweighing the variability associated with crural length.

303 Without semi-landmarks, the variation of the medial edge among Recent crural morphs is not
304 captured fully. This suggests that the shape and curvature of the medial edge, in all three
305 dimensions, is particularly important for distinguishing Recent crural morphs. Delineating
306 Recent crural morphs depends on the degree of medial twisting from proximal to distal ends of
307 the crura, a transformation that is expressed ontogenetically.

308 Statistical analyses of landmark and semi-landmark coordinates for all adult individuals
309 indicate that those with the same crural morph generally occupy a volume of morphospace that is
310 restricted relative to the separation between groups of different crural morphologies. The
311 canaliform crural morph is an exception (Fig. 5), in that it consistently groups with the
312 raduliform crura, supporting the grouping of both these crural morphs into the raducal group.
313 The Euclidean distance between *Notosaria* and *Hemithiris* (calculated from the first ten PC
314 scores), both considered to have raduliform crura, are as different from one another as are most
315 crural morphs from one another (Fig. 5). Canaliform crura only overlap with the raduliform crura
316 of *Notosaria*, not those of *Hemithiris* (Fig. 5).

317 Major axes of shape variation are potentially related to size; therefore we performed a
318 multivariate regression analysis to test the degree of association between crural centroid size and
319 the first three principal components of the landmark and semi-landmark analysis. The analysis
320 shows that there is no general dependence between size and shape (R^2 = ; p = x), but crural size
321 and PC 1 are significantly correlated. The linear dependence of PC 1 on size indicates that it
322 describes allometric size-related variation (among adults) among the crural morphs (R^2 = 0.20; p
323 = 0.03). The dependence, however, is not a uniform one among morphs, but instead is a function
324 of the exceptional differences of the small-sized *Neorhynchia profunda* crura and the larger
325 *Basiliola lucida* crura from an otherwise isometric similarity among the remaining taxa. Size is

not correlated significantly with PC 2 (R^2 = 0.12; p = 0.11) or PC 3 (R^2 = 0.001; p = 0.87). Comparing a simple linear measure of crural length with overall shell length (Fig. 6A), it is clear that smaller individuals, in general, have shorter crura than larger individuals, as might be expected. And yet, the relationship between centroid size of the crural region and overall shell length among all species is not necessarily as clear; adults of species in some genera (e.g., *Pemphixina*) have a much different allometric relationship between crural region and shell length than closely-related adults of the same shell length in other genera (Fig. 6B).

Within-Morph Variability.—Previous authors (Rothpletz 1886; Muir-Wood 1934; Wisniewska 1932; Cooper 1959; Ager 1965; Savage et al. 2002; among others) have noted the variable morphology of the raduliform morph, including variation in size, distal end morphology, and angle of curvature. We performed a second PCA of the landmark and semi-landmark coordinates of the raduliform crura in adult *Notosaria nigricans* and *Hemithiris psittacea* specimens only, to investigate within morph variability among species (Fig. 7). PC 1 accounts for 64.93% of the total variance in the data. The crura of *Notosaria nigricans* are thicker and more robust than those in *Hemithiris psittacea,* even though they have the same curvature and distal tip morphology. This PCA, along with the Procrustes distance information, supports the results of the all-adult crural morph PCA (Fig. 5), which illustrates that the two raduliform species are as different from one another as are any two different morphs, as discussed earlier. It is unclear whether other morphs might exhibit comparable variability; additional species per morph are being investigated currently to test this possibility as are additional adults in other species with raduliform crura.

Crural "Cognate" Groups.—We used the results of the PCA of landmarks and semi-landmarks on adults to test the morphological integrity of the four crural groups proposed by

Manceñido et al. (2007) (Fig. 2, 5). PC 1 and PC2 (Fig. 5A) separate representatives of the four groups from one another; PC 1 and PC 3 separate the septifal and arcual groups from the others, but the ensimergal and some members of the raducal group overlap one another completely. Representatives of the arcual group (spinuliform and arcuiform crura) occupy two distinct areas of morphospace (Fig. 5). The raducal group (canaliform and raduliform crura) shows a similar pattern, with the greatest separation between the two raduliform species, as noted above. This suggests that these two groups are not necessarily morphologically cohesive and the variation between raduliform species is as great as, or greater than, that between two different morphs. However, the crural groups put forth by Manceñido et al. (2007) and Manceñido and Motchurova-Dekova (2010) appear to be grouped mainly according to hypothesized evolutionary transformations, not necessarily morphological cohesion, so it is perhaps not unexpected that the crural morphs placed in one group do not cluster in statistical space.

Cluster Analysis of Adults.—Single linkage and neighbor-joining cluster analyses of the Euclidean distances between adults in principal component space consistently generated four main clusters (Fig. 8). Individuals with the same crural morph cluster together, as expected from the distributions in Fig. 5, with one exception. *Pemphixina* (canaliform) clusters with *Notosaria* (raduliform), while *Hemithiris* (raduliform) clusters with *Basiliola* (falciform); these two clusters themselves cluster together more closely than do either of the other two clusters. *Frieleia* (spinuliform) and *Cryptopora* (maniculiform) form the third main cluster, and *Neorhynchia* (arcuiform) forms a cluster that is most dissimilar to all the others. The current landmark configuration was unable to capture the serrated distal end of the maniculiform crura, a feature that distinguishes them from all other crural types.

371 *Summary of Results*.—Crura vary in their morphology among adults within a single
372 species, genus, or superfamily, among adults in different species assigned to the same crural
373 morph, and among adults assigned to different crural morphs. Adult individuals in the same
374 species, having the same crural morph, typically cluster together in the shape space defined here.
375 Groups of morphs recognized previously (Manceñido and Motchurova-Dekova 2010) are often
376 but not always distinct from one another in this morphospace. Data on more species representing
377 the only six extant crural morphs are needed to test this conclusion more rigorously.

378 **Discussion**

379 Crura are a fundamentally important feature of all rhynchonellate brachiopods (sensu
380 Williams et al. 1996; Williams and Carlson 2007) because they function to support the
381 lophophore within the mantle cavity. Crura first appear, phylogenetically, in derived
382 syntrophiidine pentamerides, the camerelloids and pentameridines, which share common
383 ancestry with the Rhynchonellida (Carlson et al. 2002). Rhynchonellida is a large, ancient
384 paraphyletic group from which the various spiralia-bearing and loop-bearing groups have
385 evolved (Carlson 2007). Because crura form the structural base of both spiralia and loops,
386 characterizing their morphological variability in ontogeny (and phylogeny) informs our
387 understanding of the evolutionary history of Neoarticulata (Carlson and Cohen in press), the
388 crown clade of articulated brachiopods. This study was designed as a preliminary test of the
389 morphological integrity of named crura types (morphs) and the grouping of crural types into
390 “cognate groups.” Our study provides a quantitative morphological foundation for more
391 comprehensive tests of hypotheses of heterochrony (currently ongoing), which have been
392 suggested to play a role in these evolutionary transformations (Manceñido and Motchurova-
393 Dekova 2010).

394 *Methodological Approach*.—The small size and delicate structure of crura have hindered
395 detailed study of their morphology for many years. MicroCT imaging techniques provide novel
396 ways to investigate the morphology of such very small features. Three-dimensional computer
397 models have been generated from CT-scanned images of extinct spire-bearing brachiopods, from
398 which physical models were made to investigate water flow through the mantle cavity (Shiino et
399 al. 2009; Shiino and Kuwazuru 2010); however, our study is the first to quantify morphological
400 variability among crura using these techniques. The traditional method of serial sectioning (e.g.,
401 Ager 1965; Motchurova-Dekova et al. 2002; Savage et al. 2002; Manceñido and Motchurova-
402 Dekova 2010) destroys shell material and thus informative morphological detail between each
403 section, which makes it difficult to interpret the complex 3D geometries of very small crura.
404 Scanning electron microscopy (SEM), a common imaging technique, yields highly resolved, but
405 static, 2D views of crura. Furthermore, in order to capture an unrestricted SEM image of the
406 cardinalia and crura, the valves must first be disarticulated, which can damage brachiopods like
407 rhynchonellides with cyrtomatodont (interlocking) hinge structures (Jaanusson 1971; Carlson
408 1989). Three-dimensional surface models created from successive, closely-spaced CT scans
409 allow the digital capture and dynamic manipulation of the entire hinge area of the brachiopod in
410 three dimensions without the need for disarticulation, so that more detailed quantitative and
411 qualitative analyses can be undertaken.

412 *Morphologic, Taxonomic, and Phylogenetic Variation Among Adult Crura*.—
413 Morphologically, the crura of adult extant rhynchonellides vary mainly in five parameters:
414 height, width, and length of each crus; degree of curvature of the entire crus, particularly along
415 the dorso-medial edge; and the angle of divergence between the two crus' (Fig. 3). Even small
416 variations in these parameters may significantly affect the position and orientation of the

417 spirolophe, and thus influence the three-dimensional geometry of water movement through the
418 mantle cavity (see Ager 1965; Rudwick 1970; LaBarbera 1977; James et al. 1992; Williams et al.
419 1997). The particular functional significance of minor variations in position and orientation has
420 not yet been investigated, and is not the focus of this study, but would yield interesting insights
421 into patterns of water flow between the valves, and the effect of those differences on
422 rhynchonellide feeding behavior among adults of different overall body size.

423 We studied multiple individuals per species, representing seven different species;
424 individuals of the same crural morph (and species) clustered together, with six of the seven
425 species clusters occupying a distinctly different region in the shape space constructed (Fig. 5).
426 Taxonomically, this confirms the morphological integrity of six of the seven species with respect
427 to crural morphology, as well as the morphological integrity of five of the six named extant
428 crural morphs. This result suggests that our original prediction — that crural morphs had been
429 oversplit — is not borne out among the six extant crural morphs. More individuals from
430 additional extant (and extinct) species must be analyzed to test these preliminary conclusions, but
431 most extant crural morphs appear to be quantitatively distinct from one another, and their relative
432 position in morphospace is now established. The exceptions to this pattern: two raduliform
433 species analyzed are as different from one another as any two other crural morphs, and
434 canaliform individuals largely overlap one of the two raduliform species clusters.

435 With respect to higher taxonomic affiliation, three of the four superfamilies form distinct
436 morphological clusters separate from the others (Fig. 5). Three species in the superfamily
437 Hemithiridoidea cluster relatively closely together in the morphospace, but the two species in
438 Norelloidea do not, which indicates that crural morphology varies among extant representatives
439 per superfamily. Several extinct superfamilies have been characterized by the same crural morph

(raduliform), while others, particularly the four superfamilies with extant representatives, are characterized by multiple morphs, rarely including raduliform. These four superfamilies might have experienced a diversification in crural morphs from a raduliform ancestral state, which may have contributed to their evolutionary success. It is also possible that we are simply better able to image and study the diversity of these crural types because some are extant.

Phylogenetically, the raduliform crural morph (Fig. 3, 7) is the most basal (Schreiber et al. 2013) among all Rhynchonellida, extant and extinct; it is also the morph that appears to be the most variable morphologically among constituent species (given our limited sampling regime so far). It is the morph that first appears stratigraphically as well (Manceñido and Owen 2001; Savage et al. 2002). Very little is known about the nature of morphological variability (both within and among species) of the stratigraphically early raduliform crura — shape of the distal ends, angle of curvature, cross-sectional shape — due to poor preservation and the difficulties of imaging crura in fossils; it has been questioned whether these early crura should even be considered raduliform (Ager 1965; Savage 1996; Savage et al. 2002). However, the presence of raduliform-like crura in many well-preserved pentameride brachiopods supports the basal phylogenetic position of raduliform crura among all the rhynchonellides (Carlson 1993; Carlson et al. 2002).

Among crown clade (extant) Rhynchonellida only, the basal members of three of the four subclades recognized in morphological phylogenetic analyses possess spinuliform crura (Fig. 3F); the fourth, raduliform (Schreiber et al. 2013: Fig. 3C). Molecular analysis of 12 species of extant rhynchonellides discovered three subclades (Cohen and Bitner 2013); basal members of each of these three subclades have either spinuliform or arcuiform (Fig. 3E) crura. Phylogenetic analyses using either type of data support similar ancestral character state reconstruction of

463 crural types among the extant taxa: spinuliform appears to be the ancestral crural morph.
464 Raduliform crura are clearly the stratigraphically oldest and most common morph, suggesting
465 that the spinuliform type evolved as a shared derived feature of the crown clade Rhynchonellida.
466 The nature of the evolutionary transition from raduliform to spinuliform crura has not yet been
467 investigated morphologically or phylogenetically in detail, but is currently under investigation.
468 It is intriguing that the cluster analysis of adult crural morphology (Fig. 8) produces a
469 branching pattern that is quite different from the current classification (Savage et al. 2002) and
470 from both recent phylogenetic analyses (Cohen and Bitner 2013; Schreiber et al. 2013). The
471 cluster analysis includes only features of crural morphology, however, while the classification
472 and the phylogenetic analyses include essentially all morphological features or a large number of
473 molecular characters simultaneously, so differences between them should perhaps be expected.
474 Furthermore, the cluster analysis is purely distance-based, and takes no account of polarity
475 determined from outgroups and the sequential acquisition of apomorphies that are suggested by a
476 phylogenetic analysis.
477 *Crural "Cognate" Groups*.—Manceñido and Motchurova-Dekova
478 (2010) organized 15 of the 17 named crural types into four groups (Fig. 2): raducal, arcual,
479 septifal, and ensimergal. There are two components to these groups: the assignment of types to a
480 particular group, based generally and qualitatively on crural morphology; and hypotheses of
481 morphological, developmental, and/or phylogenetic transformations between types. With respect
482 to the first component, our main focus in this study, we predicted that, based on the work of
483 Manceñido and Motchurova-Dekova (2010), crural morphs in the same group would cluster
484 together morphologically, and that crural groups would be separate from one another in the shape
485 space constructed. Our results reveal that some morphs cluster together by group, but others do

not. Crural morphs in three of the four named crural groups do occupy distinctly different regions of shape space (Fig. 5), but more than one morph in each of only two groups were investigated, necessarily so since our study focused on extant species of which only six of the 17 types are represented. Raduliform and canaliform morphs cluster together as predicted (Fig. 8), but falciform morphs cluster with them as well, which is not consistent with our predictions. Spinuliform and arcuiform morphs do not cluster together, as we predicted that they would. Morphometric analyses of additional species representing each morph are clearly required to test the generality of these preliminary findings, but it appears that most (not all) crural groups are quantitatively distinct, supporting the morphological distinctions among these “cognate” crural groups.

As described by Manceñido and Motchurova-Dekova (2010), the configuration of crural groups provides a rich source of evolutionary hypotheses to test, many of which involve heterochrony, or the evolutionary consequences of changes in developmental rate or timing, leading to changes in size and shape from ancestor to descendant. Three distinct types of information are required in order to test hypotheses of heterochrony: qualitative and quantitative data on size and shape; data on the nature of and sequence of developmental transformations over ontogeny; and phylogenetic hypotheses that enable comparisons between putative ancestors and descendants (minimally, identification of sister group pairs). As noted previously, this study is focused primarily on establishing a foundation based on the first of these three types of data.

Conclusion

Crura are a fundamentally important feature of all crown clade articulated brachiopods because they function to support the lophophore within the mantle cavity. Crura form the structural base of both spiralia and loops and studying their morphological variation can give us

valuable insights in the evolutionary history of crown clade articulated brachiopods. Our study provides a quantitative morphological foundation for more comprehensive tests of possible mechanisms (e.g., heterochrony) generating the evolutionary changes we see.

MicroCT imaging techniques provide novel ways to investigate the morphology of very small “hidden” features, such as the crura. Three-dimensional surface models created from CT scans allow the digital capture and dynamic manipulation of the entire hinge area of the brachiopod in three dimensions, allowing more detailed quantitative and qualitative analyses to be undertaken.

Morphologically, the crura of adult extant rhynchonellides vary primarily in five parameters: height, width, and length of each crus; degree of curvature of the entire crus, particularly along the dorso-medial edge; and the angle of divergence between the two crus’. This study confirms the morphological integrity of six of the seven species with respect to crural morphology, as well as the morphological integrity of five of the six named extant crural morphs; extant crural morphs at least do not appear to have been oversplit. However, the two raduliform species analyzed are as different from one another as any two other crural morphs, and canaliform individuals largely overlap one of the two raduliform species clusters. Furthermore, three of the four superfamilies form distinct morphological clusters separate from the others. Stratigraphically and phylogenetically, the raduliform crural morph is the most basal among all Rhynchonellida, extant and extinct; it is also the morph that appears today to be the most variable morphologically among constituent species.

Crural morphs in three of the four named crural cognate groups occupy distinctly different regions of morphometric shape space, supporting the qualitative morphological

distinctions among them, but sampling of additional species in the morphs and groups must be increased to test these preliminary results.

Acknowledgments

We thank R. Motani for helpful discussions and advice throughout this project, which grew out of one portion of the first author's dissertation research. Anonymous reviewers provided helpful suggestions that improved the quality of the manuscript. We also thank Scripps Institution of Oceanography, California Academy of Sciences, and D. E. Lee (University of Otago, New Zealand) for access to specimens. We thank J. Thompson (National Museum of Natural History) for providing access to specimens, and other assistance during research visits. Finally, we thank Tanya Garcia-Nolan (J.D. Wheat Veterinary Orthopedic Research Laboratory at the University of California, Davis School of Veterinary Medicine) for all microCT scanning of specimens. We gratefully acknowledge support for this project provided by National Science Foundation grant EAR 1147537. Support for this research was also provided by Durrell funds from the Department of Geology, University of California, Davis, and a Geological Society of America Graduate Student Research Grant to the first author.

Literature Cited

Abel, R. L., C. R. Laurini, and M. Richter. 2012. A palaeobiologist's guide to "virtual" micro-CT preparation. Palaeontologia Electronica 15(2):palaeo-electronica.org/content/issue-2-2012-technical-articles/233-micro-ct-workflow.

Ager, D. V. 1962. A monograph of the British Liassic Rhynchonellidae. Part III. Palaeontographical Society of London, Monograph 116(498):85–136.

———. 1965. Mesozoic and Cenozoic Rhynchonellacea. Pp. H597–H625 *in* R. C. Moore, ed. Treatise on invertebrate paleontology. Part H, Brachiopoda. Geological Society of America and University of Kansas Press. Lawrence.

Alberch, P., S. J. Gould, G. F. Oster, and D. B. Wake. 1979. Size and shape in ontogeny and phylogeny. Paleobiology 5:296–317.

Angiolini, L., V. Barberini, N. Fusi, and A. Villa. 2010. The internal morphology of fossil brachiopods under x-ray computed tomography (CT). I*n* Program & Abstracts, 6th International Brachiopod Congress, Geological Society of Australia Abstracts 95:7.

Baranov, V. V. 1980. Morphology of crura and new rhynchonellid taxa. Paleontologicheskii Zhurnal 4:75-90.

Bookstein, F. L. 1991. Morphometric tools for landmark data. Cambridge University Press, Cambridge, U.K.

———. 1997. Landmark methods for forms without landmarks: morphometrics of group differences in outline shape. Medical Image Analysis 1(3):225–243.

Boucot, A. J. and R. A. Wilson. 1994. Origin and early radiation of terebratuloid brachiopods: thoughts provoked by *Prorensselaeria* and *Nanothyris*. Journal of Paleontology 68(5):1002–1025.

Brunton, C. H. C., F. Alvarez, and D. I. MacKinnon. 1996. Morphological terms used to describe the cardinalia of articulate brachiopods: homologies and recommendations. Historical Biology 11:9–41.

Carlson, S. J. 1989. The articulate brachiopod hinge mechanism: morphological and functional variation. Paleobiology 15(4):364–386.

———. 1993. Phylogeny and evolution of ‘pentameride’ brachiopods. Palaeontology 36:807–837.

———. 1995. Phylogenetic relationships among extant brachiopods. Cladistics 11:131–197.

———. 2007. Recent research on brachiopod evolution. Pp. H2878–H2900 *in* A. Williams et al. Brachiopoda 6 (revised), Supplement. Part H of P. A. Seldon, ed. Treatise on invertebrate paleontology. Geological Society of America, Boulder and University of Kansas, Lawrence.

———. 2012. Are phylogenetic nomenclature and invertebrate paleontology friends or foes? Geological Society of America Annual Meeting, Abstracts with Programs 44(7):34.

Carlson, S. J. and L. R. Leighton. 2001. The phylogeny and classification of Rhynchonelliformea. The Paleontological Society Papers 7:27–51.

Carlson, S. J. and B. L. Cohen. In press 2013. *Neoarticulata*. *in* K. de Queiroz, P. D. Cantino, and J. A. Gauthier, eds. Phylonyms: a companion to the PhyloCode. University of California Press, Berkeley and Los Angeles.

Carlson, S. J., A. J. Boutcot, R. Jia-Yu, R. B. Blodgett. 2002. Pentamerida. Pp. H922–H1027 *in* A. Williams et al. Brachiopoda 4 (revised), Rhynchonelliformea (part). Part H of R. L. Kaesler, ed. Treatise on invertebrate paleontology. Geological Society of America, Boulder and University of Kansas Press, Lawrence.

Cohen, B. L. 2001a. Brachiopod molecular phylogeny advances. *In* C. H. C. Brunton, L. R. M. Cocks, and S. Long, eds. Brachiopods past and present. Proceedings of the Millennium Brachiopod Congress, 2000. The Systematics Association Special Volume Series 63:121–128. Taylor and Francis. London.

———. 2001b. Genetics and molecular systematics of brachiopods. *In* S. J. Carlson and M. R. Sandy, eds. Brachiopods ancient and modern. A Tribute to G. Arthur Cooper.7:53–67. Paleontological Society, Pittsburgh.

———. 2007. The brachiopod genome. Pp. H2356–H2372 *in* A. Williams et al. Brachiopoda 6 (revised), Supplement. Part H of P. A. Seldon, ed. Treatise on invertebrate paleontology. Geological Society of America, Boulder and University of Kansas, Lawrence.

Cohen, B. L. and M. A. Bitner. 2013. Molecular phylogeny of rhynchonellide articulate brachiopods (Brachiopoda, Rhynchonellida). Journal of Paleontology 87(2):211–216.

Cohen, B. L. and A. B. Gawthrop. 1997. The brachiopod genome. Pp. H189–H211 *in* A. Williams et al. Brachiopoda 1 (revised), Introduction. Part H of R. L. Kaesler, ed. Treatise on invertebrate paleontology. Geological Society of America, Boulder and University of Kansas, Lawrence.

Cohen, B. L. and A. Weydmann. 2005. Molecular evidence that phoronids are a subtaxon of brachiopods (Brachiopoda: Phoronata) and that genetic divergence of metazoan phyla began long before the Early Cambrian. Organisms, Diversity and Evolution 5(4):253–273.

Cooper, G. A. 1959. Genera of Tertiary and recent rhynchonelloid brachiopods. Smithsonian Miscellaneous Collections 139(5):1–90.

———. 1972. Homeomorphy in Recent deep-sea brachiopods. Smithsonian Contributions to Paleobiology, 11:1–15.

645 Dagys, A. S. 1968. Iurskie i rannemelovye brakhiopody severa Sibiri [Jurassic and Early
646 Cretaceous brachiopods from north Siberia]. Trudy Instituta Geologii I Geofiziki 41:1–
647 167.
648
649 Dall, W. H. 1895. Report on Mollusca and Brachiopoda dredged in deep water, chiefly near the
650 Hawaiian Islands, with illustrations of hitherto unfigured species from northwest
651 America. Proceedings of the United States National Museum 17(1032):675–733.
652
653 Davidson, T. 1880. Report on the Brachiopoda dredged by H. M. S. Challenger during the years
654 1873–1876. Report of scientific results of the Voyage H.M.S. Challenger (Zoology) 1:1–
655 67.
656
657 Elliott, J. C. and S. D. Dover. 1982. X-ray microtomography. Journal of Microscopy 126:211–
658 213.
659
660 Emig, C. C. 1992. Functional disposition of the lophophore in living Brachiopoda. Lethaia
661 25:291–302.
662
663 Flannery, B. P., H. W. Deckman, W. G. Roberge, and K. L. D'Amico. 1987. Three-dimensional x-
664 ray microtomography. Science 237:1439–1444.
665
666 Gering D, A. Nabavi, R. Kikinis, W. Grimson, N. Hata, P. Everett, F. Jolesz, and W. Wells. 1999.
667 An Integrated visualization system for surgical planning and guidance using image fusion

and interventional imaging. International Conference on Medical Image Computing and Computer Assisted Intervention 2:809–819.

Gmelin, J. F. 1790. Systema naturae, editio decimal tertia aucta. Reformata I. Ps. VI. Vermes. Lipsiae. Pp. 3021–4120.

Görög, Á., B. Szinger, E. Tóth, and J. Viszkok. 2012. Methodology of the micro-computer tomography on foraminifera. Palaeontologia Electronica 15(1). palaeo-electronica.org/content/issue-1-2012-technical-articles/121-methodology-of-ct-on-forams

Gould, A. A. 1862. Descriptions of shells and molluscs from 1839–1862 *Ostia conchologia.* Boston, 256 p.

Gower, J. C. 1975. Generalized Procrustes analysis. Psychometrika 40:33–51.

Gunz, P. 2001. Using semi-landmarks in three dimensions to model human neurocranial shape (Master Thesis, University of Vienna, Vienna, 2001).

———. 2005. Statistical and geometric reconstruction of hominid crania: reconstructing australopithecine ontogeny (Ph.D. Thesis, University of Vienna, Vienna, 2005).

689 Gunz, P., P. Mitteroecker, and F. L. Bookstein. 2005. Semi-landmarks in three dimensions. Pp.
690 73–98 *in* D. E. Slice , ed. Modern morphometrics in physical anthropology. Kluwer
691 Academic/Plenum Publishers, New York.
692
693 Hammer, Ø. and D. A. T. Hammer and P. D. Ryan. 2001. PAST: paleontological statistics
694 software package for education and data analysis. Palaeontologica Electronica 4(1):9.
695
696 Holmer, L. E. and L. Y. Popov. 2000. Lingulata. Pp. H30–H146 *in* A. Williams et al.
697 Brachiopoda 2 (revised), Linguliformea, Craniiformea, and Rhynchonelliformea (part).
698 Part H of R. L. Kaesler, ed. Treatise on invertebrate paleontology. Geological Society of
699 America and University of Kansas Press, Lawrence.
700
701 Jaanusson, V. J. 1971. Evolution of the brachiopod hinge. Smithsonian Contributions to
702 Paleobiology 3:33–46.
703
704 James, M., A. D. Ansell, M. J. Collins, G. B. Curry, L. S. Peck, and M. C. Rhodes. 1992. Biology
705 of living brachiopods. Advances in Marine Biology 28:175–387.
706
707 Jeffreys, J. G. 1876. On some new and remarkable North-Atlantic Brachiopoda. Annals and
708 Magazine of Natural History (series 4) 18:250–253.
709

Ketcham R. A. and W. D. Carlson. 2001. Acquisition, optimization and interpretation of x-ray computed tomographic imagery: applications to the geosciences. Computers and Geosciences 27:381–400.

Kuhn, O. 1949. Lehrbuch der Paläozoologie. E. Schweizerbart'sche Verlagsbuchhandlung. Stuttgart.

LaBarbera, M. 1977. Brachiopod orientation to water movement 1. theory, laboratory behavior, and field orientations. Paleobiology 3(3):270–287.

———. 1978. Brachiopod orientation to water movement, functional morphology. Lethaia 11(1):67–79.

———. 1981. Water flow patterns in and around three species of articulate brachiopods. Journal of Experimental Marine Biology and Ecology 55:185–206.

Lee, D. E. and J. B. Wilson. 1979. Cenozoic and recent rhynchonellide brachiopods of New Zealand–systematics and variation in the genus *Notosaria*. Journal of the Royal Society of New Zealand 9(4):437–463.

Logan, A. 2007. Geographic distribution of extant articulated brachiopods. Pp. H3083–H3115 *in* A. Williams et al. Brachiopoda 6 (revised), Supplement. Part H of P. A. Seldon, ed.

Treatise on invertebrate paleontology. Geological Society of America, Boulder and University of Kansas, Lawrence.

Long, J. A. and S. A. Stricker. 1991. Brachiopoda. *In* A. Geise, J. S. Pearse, and V. B. Pearse, eds. Reproduction of Marine Invertebrates 6:47–84.

Manceñido, M. O. 1998. Revaluación de los tipos de crura de los Rhynchonellida post-paleozoicos (Brachiopoda). – VII Congreso Argentino de Paleontología y Biostratigrafía, Resúmenes. Bahía Blance, Argentina. p. 46.

———. 2000. Crural types among Post-Paleozoic Rhynchonellida (Brachiopoda). The Millenium Brachiopod Congress, 10-14 July 2000. London, Abstracts. The Natural History Museum, London, p. 57.

Manceñido, M. O. and E. F. Owen. 2001. Post-Paleozoic Rhynchonellida (Brachiopoda): classification and evolutionary background. Pp. 189–200 *in* L. R. M. Cocks, C. H. C. Brunton, and S. L. Long, eds. Brachiopods past and present. Proceedings of the Millennium Brachiopod Congress, 2000. The Systematics Association Special Volume Series, Taylor and Francis, London.

Manceñido, M. O. and N. Motchurova-Dekova. 2010. A review of crural types, their relationships to shell microstructure, and significance among post-Paleozoic

754 Rhynchonellida. Evolution and Development of the Brachiopod, Special Papers in
755 Palaeontology Series 84:203–204.
756
757 Manceñido, M. O., E. F. Owen, and D.-L. Sun. 2007. Post-Paleozoic Rhynchonellida. Pp.
758 H2727–2741 *in* A. Williams et al. Brachiopoda 6 (revised), Supplement. Part H of P. A.
759 Seldon, ed. Treatise on invertebrate paleontology. Geological Society of America,
760 Boulder and University of Kansas, Lawrence.
761
762 Mitteröcker P. and P. Gunz. 2002. Semi-landmarks on curves and surfaces in three dimensions.
763 American Journal of Physical Anthropology. Supplement 34:114–115.
764
765 ———. 2009. Advances in geometric morphometrics. Evolutionary Biology 36:235–247.
766
767 Monnet, C., C. Zollikofer, H. Bucher, and N. Goudemand. 2009. Three-dimensional
768 morphometric ontogeny of mollusc shells by micro-computed tomography and geometric
769 analysis. Palaeontologia Electronica 12(3).
770 http://palaeo-electronica.org/2009_3/183/index.html
771
772 Motchurova-Dekova, N., M. Saito, and K. Endo. 2002. The Recent rhynchonellide brachiopod
773 *Parasphenarina cavernicola* gen. et sp. nov. from the submarine caves of Okinawa,
774 Japan. Paleontological Research 6:299–319.
775

776 Muir-Wood, H. M. 1934. On the internal structure of some Mesozoic Brachiopoda. Philosophical
777 Transactions of the Royal Society of London (Series B) 223:511–567.
778
779 O'Higgins P. and N. Jones. 1998. Facial growth in *Cercocebus torquatus*: An application of
780 three dimensional geometric morphometric techniques to the study of
781 morphological variation. Journal of Anatomy 193:251–272.
782
783 Pakhnevich, A. V. 2010. Micro-CT investigations of Recent and fossil brachiopods. *In* Program
784 and Abstracts, 6th International Brachiopod Congress, 1-5 February 2010,
785 Melbourne,Australia; Geological Society of Australia Abstracts 95:85
786
787 Peck, R. L., J. B. Bailey, R. J. Heck, N. T. Scaiff. 2009. X-ray CT scan as an aid to identification
788 and description of a new bivalve species (Mollusca) from the Mississippian Bluefield
789 formation, southeastern West Virginia. Journal of Paleontology 83(6):954–961.
790
791 Pieper S., M. Halle, R. Kikinis. 2004. 3D SLICER. Proceedings of the 1st IEEE International
792 Symposium on Biomedical Imaging: From Nano to Macro 1:632–635.
793
794 Pieper S., B. Lorensen, W. Schroeder, R. Kikinis. 2006. The NA-MIC Kit: ITK, VTK,
795 pipelines, grids and 3D Slicer as an open platform for the medical image computing
796 community. Proceedings of the 3rd IEEE International Symposium on Biomedical
797 Imaging: From Nano to Macro 1:698–701.
798

Popov, L. Y., M. G. Bassett, and L. E. Holmer. 2000. Craniata. Pp. H158–H168 *in* A. Williams et al. Brachiopoda 2 (revised), Linguliformea, Craniiformea, and Rhynchonelliformea (part). Part H of R. L. Kaesler, ed. Treatise on invertebrate paleontology. Geological Society of America, Boulder and University of Kansas Press, Lawrence.

Rohlf, F. J. and D. E. Slice. 1990. Extensions of the Procrustes method for the optimal superimposition of landmarks. Systematic Zoology 39:40–59.

Rothpletz, A. 1886. Geologisch-palaeontologische monographie der bilser Alpen mit besonderer Berucksichtigung der Brachiopoden-systematik. Palaeontographica 33:1–180.

Roopnarine, P. D. 2001. Testing the hypothesis of heterochrony in morphometric data: lessons from a bivalved mollusk. Pp. 271–303 *in* M. Zelditch, ed. Beyond heterochrony: the evolution of development. Wiley-Liss.

Rudwick, M. J. S. 1970. Living and fossils brachiopods. Hutchinson and Company, London.

Savage, N. M. 1996. Classification of Paleozoic rhynchonellide brachiopods. Pp. 249–260 *in* P. Copper and J. Jin, eds. Brachiopods. Proceedings of the third International brachiopod congress, 1995. A.A. Balkema, Rotterdam.

———. 2007. Rhynchonellida (part). Pp. H2703–2716 *in* A. Williams et al. Brachiopoda 6 (revised), Supplement. Part H of P. A. Seldon, ed. Treatise on invertebrate paleontology. Geological Society of America, Boulder and University of Kansas, Lawrence.

Savage, N. M, M. O. Manceñido, E. F. Owen, S. J. Carlson, R. E. Grant, A. S. Dagys, and S. Dong-Li. 2002. Rhynchonellida. Pp. H1027–H1040 *in* A. Williams et al. Brachiopoda 4 (revised), Rhynchonelliformea (part). Part H of R. L. Kaesler, ed. Treatise on invertebrate paleontology. Geological Society of America, Boulder and University of Kansas Press, Lawrence.

Schreiber, H. A., M. A. Bitner, and S. J. Carlson. 2013. Morphological analysis of phylogenetic relationships among extant rhynchonellide brachiopds. Journal of Paleontology 87(4):550–569.

Shiino, Y. and O. Kuwazuru. 2010. Functional adaptation of spiriferide brachiopod morphology. Journal of Evolutionary Biology 23(7):1547–1557.

Shiino, Y., O. Kuwazur, and N. Yoshikawa. 2009. Computational fluid dynamics simulations on a Devonian spiriferid *Paraspirifer bownockeri* (Brachiopoda): generating mechanism of passive feeding flows. Journal of Theoretical Biology 259:132–141.

Sowerby, G. B. 1846. Descriptions of thirteen new species of brachiopods. Proceedings of the Zoological Society of London 14:91–95.

van Dam, J. A., J. Fortuny, and L. J. van Ruijven. 2011. MicroCT-scans of fossil micromammal teeth: re-defining hypsodonty and enamel proportion using true volume. Palaeogeography, Palaeoclimatology, Palaeoecology 311:103–110.

Westbroek, P. 1968. Morphological observations with systematic implications on some Paleozoic Rhynchonellida from Europe, with special emphasis on the Uncinulidae. Leidse Geologische Mededelingen 41:1–82.

Wiley, D. F., N. Amenta, D. A. Alcantara, D. Ghosh, Y. J Kil, E. Delson, W. Harcourt-Smith, F. J.Rohlf, K. St. John, B. Hamann. 2005 (2007 update). Evolutionary Morphing *in* Proceedings of IEEE Visualization 2005.

Williams, A. and S. J. Carlson. 2007. Affinities of brachiopods and trends in their evolution. Pp. H2823–H2877 *in* A. Williams et al. Brachiopoda 6 (revised), Supplement. Part H of P. A. Seldon, ed. Treatise on invertebrate paleontology. Geological Society of America, Boulder and University of Kansas, Lawrence.

Williams, A., S. J. Carlson, C. H. C. Brunton, L. E. Holmer, and L. E. Popov. 1996. A supra-ordinal classification of the Brachiopoda. Philosophical Transactions of the Royal Society of London (series B) 351:1171–1193.

Williams, A., C. H. C Brunton, and D. I. MacKinnon. 1997. Morphology Pp. H321–H440 *in* A. Williams et al. Brachiopoda 1 (revised), Introduction. Part H of R. L. Kaesler, ed. Treatise

on invertebrate paleontology. Geological Society of America, Boulder and University of Kansas, Lawrence.

Williams, A., S. J. Carlson, C. H. C. Brunton. 2000a. Brachiopod classification Pp. H1–H29 *in* A. Williams et al. Brachiopoda 2 (revised), Linguliformea, Craniiformea, and Rhynchonelliformea (part). Part H of R. L. Kaesler, ed. Treatise on invertebrate paleontology. Geological Society of America, Boulder and University of Kansas Press, Lawrence.

———. 2000b. Rhynchonelliformea Pp. H193 *in* A. Williams et al. Brachiopoda 2 (revised), Linguliformea, Craniiformea, and Rhynchonelliformea (part). Part H of R. L. Kaesler, ed. Treatise on invertebrate paleontology. Geological Society of America, Boulder and University of Kansas Press, Lawrence.

Wisniewska, M. 1932. Les Rhynchonellides du Jurassique sup. de Pologne [Rhynchonellidae Gornej Jury w Polsce]. Palaeontologia Polonica 2(1): viii + 1–71.

Zelditch, M. R., D. L. Swiderski, H. D. Sheets, and W. L. Fink, eds. 2004. Geometric morphometrics for biologists: a primer. Elsevier Press, San Diego.

Figure Captions

Figure 1. A, Generalized rhynchonellide dorsal valve (interior of posterior portion) based on *Trigonirhynchia pareti*. Adapted from Westbroek (1968) and Savage et al. (2002). B, Interior of ventral valve; C, Interior of dorsal valve; and D, Posterior of dorsal valve interior of *Hemithiris psittacea*, showing crura. Modified from Savage et al. (2002).

Figure 2. The four named crural cognate groups (Manceñido and Motchurova-Dekova 2010) and their constituent crural morphs, with arrows indicating hypothesized evolutionary transformations between. The six crural morphs present in extant rhynchonellides are denoted by asterisks; all others are found in extinct rhynchonellides. The ciliform and maniculiform crural morphs have been designated as members of the ensimergal group, but are not included in any hypothesized evolutionary relationships (Manceñido and Motchurova-Dekova 2010). Each pair of drawings per crural type represents, on the left, a view looking into the posterior interior of the dorsal valve; on the right, a lateral view of articulated valve posterior, with the dorsal valve on the right. Crural figures are modified from Savage et al. (2002).

Figure 3. Three-dimensional surface models of posterior region of dorsal valve interiors of all extant crural morphs. Models include the truncated teeth sitting in the sockets of each specimen. A, maniculiform crura of *Cryptopora gnomon;* B, falciform crura of *Basiliola lucida;* C, raduliform crura of *Hemithiris psittacea;* D, canaliform crura of *Pemphixina pyxidata;* E, arcuiform crura of *Neorhynchia profunda;* F, spinuliform crura of *Frieleia halli*. Scale bars are 1 mm. See the 3D Brachiopod Images website

912 (http://3dbrachiopodimages.ucdavis.edu/index.html) for complete 3D models of the
913 rhynchonellide crura.

914

915 Figure 4. A, Illustrations of the posterior region of the dorsal valve; B, lateral view of articulated
916 valves; and C, mid-crura transverse cross-section of a raduliform morph with dorsal valve
917 uppermost. Geometrically homologous landmarks (numbered black dots) and semi-landmarks
918 (open dots) for three-dimensional morphometric analysis. Semi-landmarks are located in relation
919 to landmarks; however, landmarks are not visible in Figure C because of the orientation of the
920 figure. Figures modified after Savage et al. (2002).

921

922 Figure 5. Results of PCA of Procrustes-fitted landmark and semi-landmark coordinates of adult
923 crural morphs. A, PC 1 versus PC 2. The morphological variation illustrated along PC 1 is
924 associated with the width of the distal end of the crus and the medial twisting of the distal end of
925 the crus. Falciform crura represent one morphological extreme with broad, medially convex
926 crura. Arcuiform crura represent the opposite extreme with narrower, twisted crura. All other
927 crural morphs plot near the origin, indicating that the width and twisting of the distal end of the
928 remaining crural morphs are very similar. The morphological variation illustrated along PC 2 is
929 associated with crus length and width. Maniculiform crura represent one end-member
930 morphology with narrow, elongated crura. Canaliform represent the opposite end-member
931 morphology with short, wide crura. Crural morphs are more or less equally distributed along PC
932 2 indicating slight variations in crural width and length among Recent crural morphs from one
933 end-member to the other. B, PC 1 versus PC 3. Morphological variation along PC 3 is associated
934 with crural curvature. Variation along PC 3 ranges from straight and laterally compressed in

spinuliform crura to dorso-ventrally compressed and ventrally curved in raduliform crura. Crural morphs are equally distributed along PC 3 indicating slight variations in crural curvature among Recent crural morphs from one extreme to the other. Members of the arcual group (arcuiform and spinuliform) do not cluster in statistical space. Members of the raducal group (raduliform and canaliform) do show overlap, but raduliform crura do not cluster tightly. Wireframe models illustrate three-dimensional end-member morphology in lateral view for each principal component. Numbered nodes on the wireframe models correspond to the measured landmarks illustrated in Figure 4. Individuals with the same crural morph are denoted with ellipses. Ellipses have no statistical meaning. A complete list of PC scores is available from the authors for all analyses.

Figure 6. A, Crura length versus shell length in juvenile and adult Recent rhynchonellides. Crura and shell length are averages estimated from at least two photographs per species in literature sources (Savage et al., 2002; Manceñido et al. 2007). Crura length is measured from base of crus to tip of crus. Shell length is the length of the ventral valve. Crura length and shell length are not significantly correlated ($r = 0.70$, $p = 0.07$). B, Centroid size versus shell length in juvenile and adult Recent rhynchonellides. Centroid size is the average centroid size of each species (the centroid size of each individual was previously calculated in this analysis). Centroid size and shell length are not significantly correlated ($r = -0.09$, $p = 0.85$) among all species.

Figure 7. PCA of raduliform crura of adult *Notosaria nigricans* and *Hemithiris psittacea.* Size has been standardized. *Notosaria* and *Hemithiris* form two distinct clusters within the raduliform

ellipse in Figure 4. Raduliform crura exhibit interspecific variability, as illustrated in this PCA. However, the one *Notosaria* outlier greatly affects the distribution of the remaining specimens. The outlier is much shorter and wider than the other specimens of *Notosaria*, indicating intraspecific variability of the crura. Variation along PC1 is associated with crural length, width, and divergence. PC 1 accounts for 64.93% of the total variance in data. The raduliform crura of *Hemithiris* tend to be more elongate, while the raduliform crura of *Notosaria* are shorter and wider. Wireframe models illustrate three-dimensional end-member morphology in lateral view for PC 1. Numbered nodes on the wireframe models correspond to the measured landmarks illustrated in Figure 4.

Figure 8. Single linkage cluster analysis of adult crura. Cluster analysis was performed using the scores on the first three principal components together. The dissimilarity measure is a measure of the Euclidean distances between specimens. Euclidean distance is a measure of the straight line distance between two points in space. Crural types tend to cluster together, with the exception of the raduliform and canaliform types. The specimens of each genus also cluster together with the exception of *Notosaria*. The one *Notosaria* individual that clusters with *Pemphixina* is the outlier in Figure 7. This *Notosaria* individual is shorter and wider than the remaining *Notosaria*.

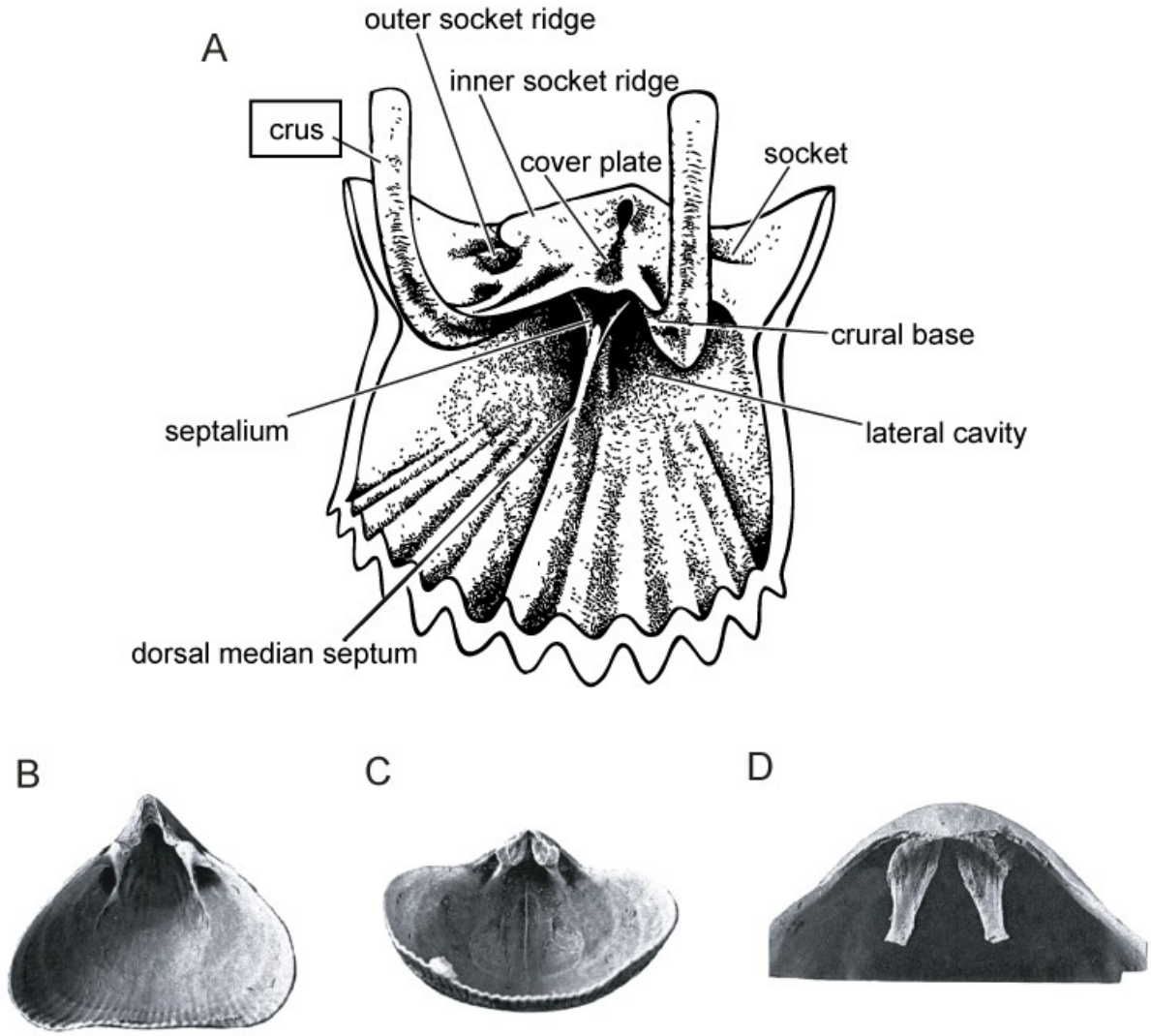

Figure 1. A, Generalized rhynchonellide dorsal valve (interior of posterior portion) based on *Trigonirhynchia pareti*. Adapted from Westbroek (1968) and Savage et al. (2002). B, Interior of ventral valve; C, Interior of dorsal valve; and D, Posterior of dorsal valve interior of *Hemithiris psittacea*, showing crura. Modified from Savage et al. (2002).

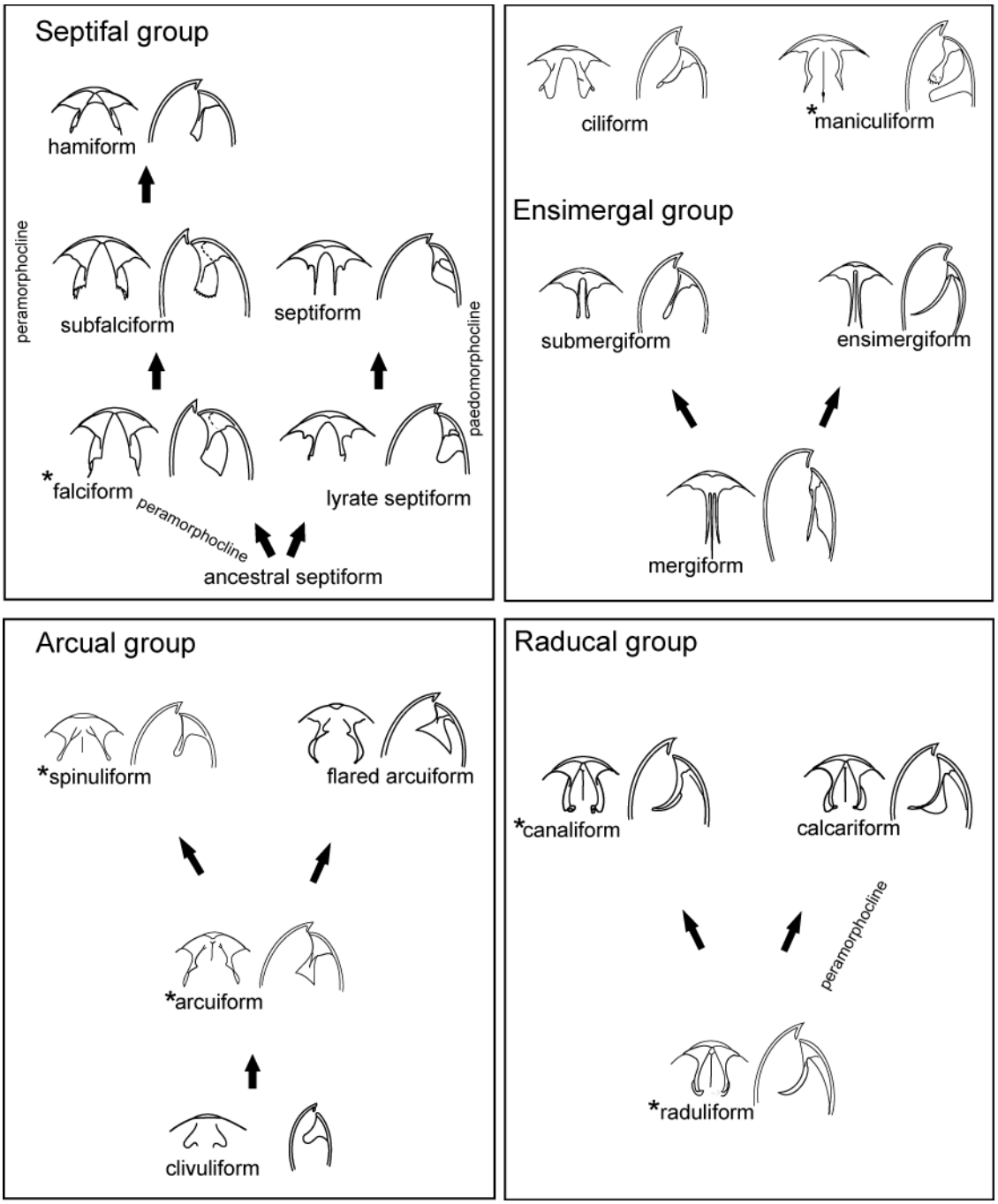

Figure 2. The four named crural cognate groups (Manceñido and Motchurova-Dekova 2010) and their constituent crural morphs, with arrows indicating hypothesized evolutionary transformations between. The six crural morphs present in extant rhynchonellides are denoted by asterisks; all others are found in extinct rhynchonellides. The ciliform and maniculiform crural morphs have been designated as members of the ensimergal group, but are not included in any hypothesized evolutionary relationships (Manceñido and Motchurova-Dekova 2010). Each pair of drawings per crural type represents, on the left, a view looking into the posterior interior of the dorsal valve; on the right, a lateral view of articulated valve posterior, with the dorsal valve on the right. Crural figures are modified from Savage et al. (2002).

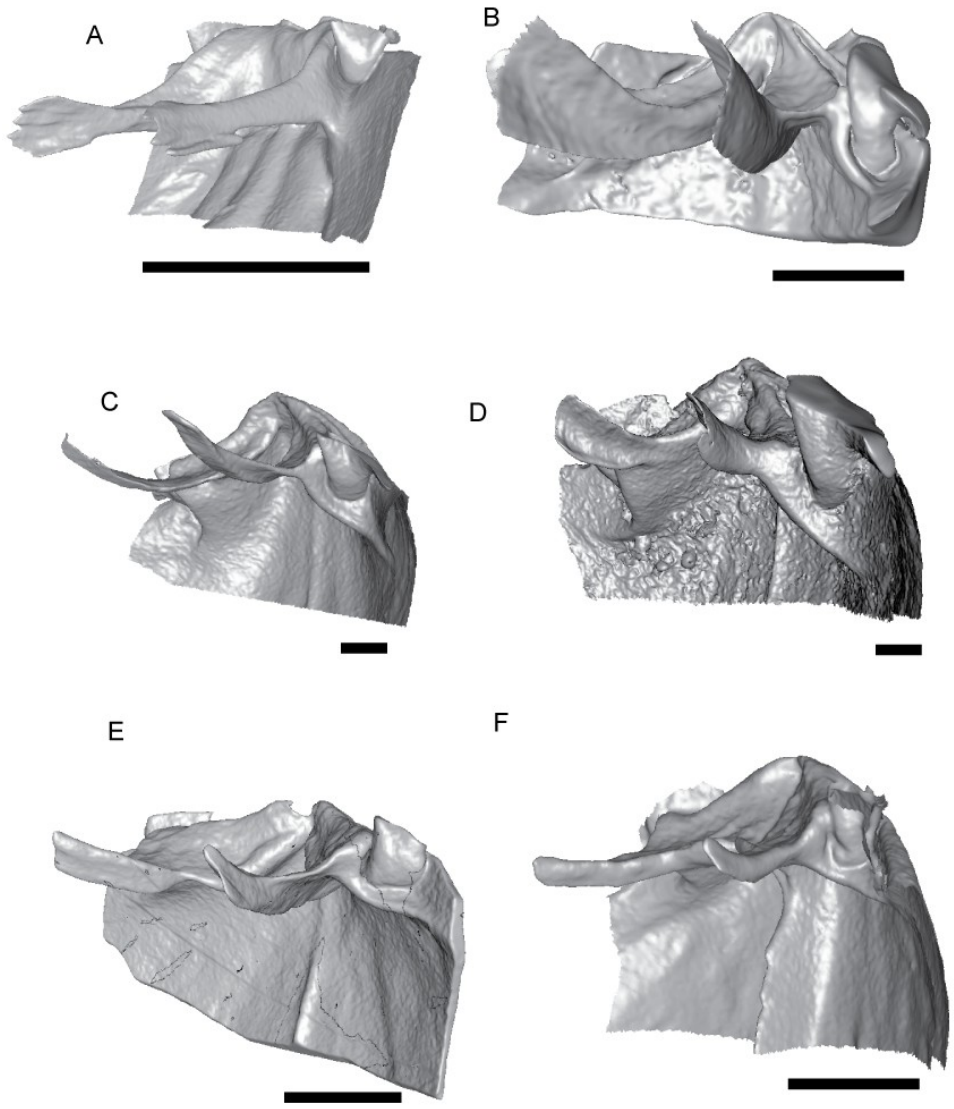

995

996

997 Figure 3. Three-dimensional surface models of posterior region of dorsal valve interiors of all
998 extant crural morphs. Models include the truncated teeth sitting in the sockets of each specimen.
999 A, maniculiform crura of *Cryptopora gnomon;* B, falciform crura of *Basiliola lucida;* C,
1000 raduliform crura of *Hemithiris psittacea;* D, canaliform crura of *Pemphixina pyxidata;* E,
1001 arcuiform crura of *Neorhynchia profunda;* F, spinuliform crura of *Frieleia halli*. Scale bars are 1
1002 mm. See the 3D Brachiopod Images website
1003 (http://3dbrachiopodimages.ucdavis.edu/index.html) for complete 3D models of the
1004 rhynchonellide crura.

1005 .

1006

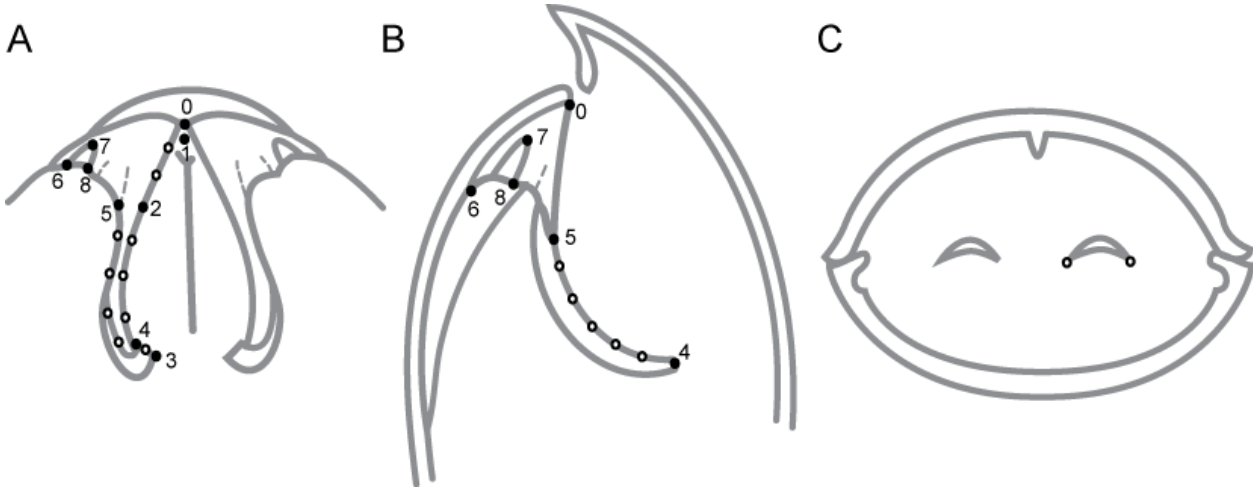

Figure 4. A, Illustrations of the posterior region of the dorsal valve; B, lateral view of articulated valves; and C, mid-crura transverse cross-section of a raduliform morph with dorsal valve uppermost. Geometrically homologous landmarks (numbered black dots) and semi-landmarks (open dots) for three-dimensional morphometric analysis. Semi-landmarks are located in relation to landmarks; however, landmarks are not visible in Figure C because of the orientation of the figure. Figures modified after Savage et al. (2002).

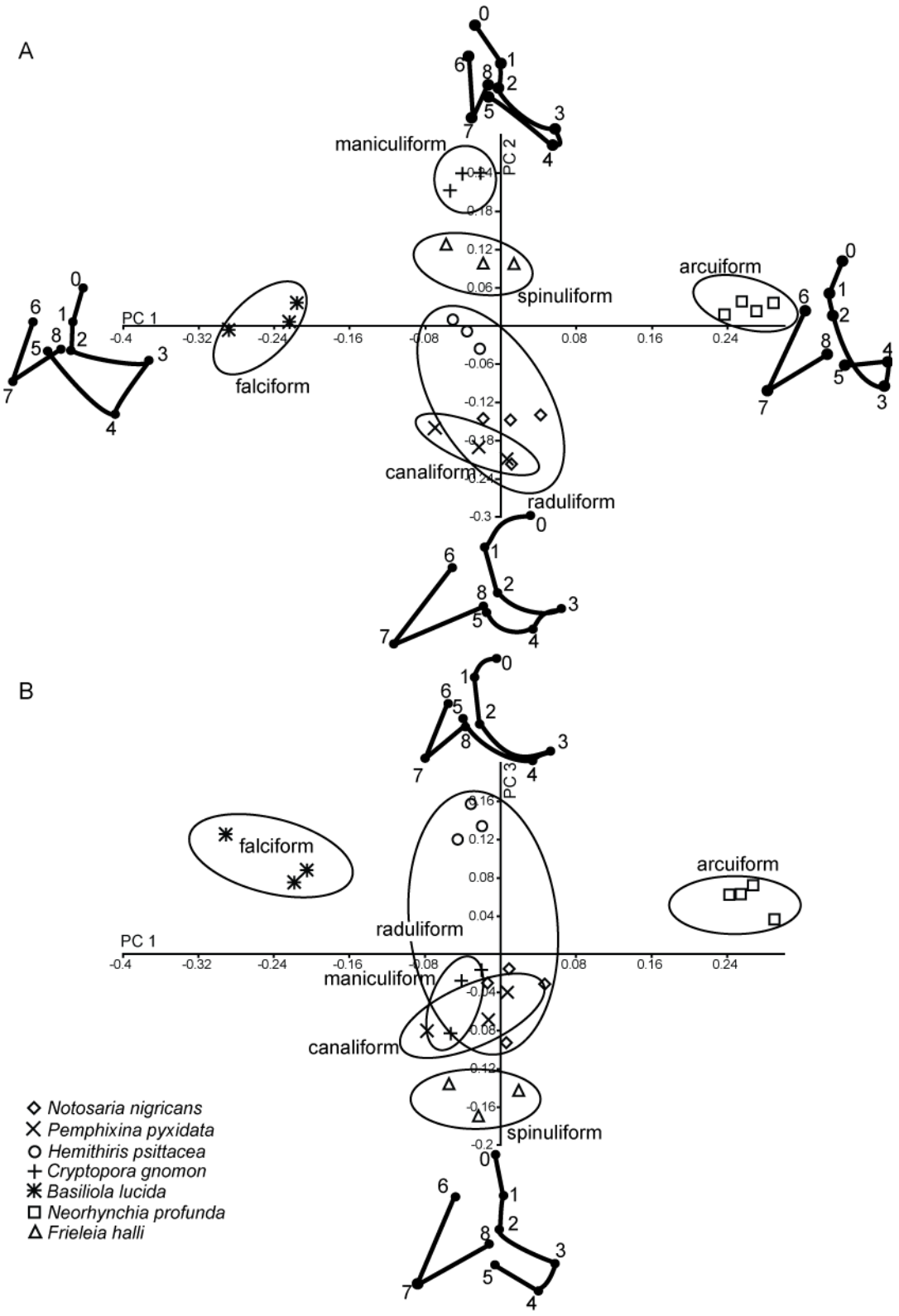
A
maniculiform
PC 2
spinuliform
arcuiform
PC 1
falciform
canaliform
raduliform
B
PC 3
falciform
arcuiform
raduliform
PC 1
maniculiform
canaliform
spinuliform
Notosaria nigricans
Pemphixina pyxidata
Hemithiris psittacea
Cryptopora gnomon
Basiliola lucida
Neorhynchia profunda
Frieleia halli

1026

1028

Figure 5. Results of PCA of Procrustes-fitted landmark and semi-landmark coordinates of adult crural morphs. A, PC 1 versus PC 2. The morphological variation illustrated along PC 1 is associated with the width of the distal end of the crus and the medial twisting of the distal end of the crus. Falciform crura represent one morphological extreme with broad, medially convex crura. Arcuiform crura represent the opposite extreme with narrower, twisted crura. All other crural morphs plot near the origin, indicating that the width and twisting of the distal end of the remaining crural morphs are very similar. The morphological variation illustrated along PC 2 is associated with crus length and width. Maniculiform crura represent one end-member morphology with narrow, elongated crura. Canaliform represent the opposite end-member morphology with short, wide crura. Crural morphs are more or less equally distributed along PC 2 indicating slight variations in crural width and length among Recent crural morphs from one end-member to the other. B, PC 1 versus PC 3. Morphological variation along PC 3 is associated with crural curvature. Variation along PC 3 ranges from straight and laterally compressed in spinuliform crura to dorso-ventrally compressed and ventrally curved in raduliform crura. Crural morphs are equally distributed along PC 3 indicating slight variations in crural curvature among Recent crural morphs from one extreme to the other. Members of the arcual group (arcuiform and spinuliform) do not cluster in statistical space. Members of the raducal group (raduliform and canaliform) do show overlap, but raduliform crura do not cluster tightly. Wireframe models illustrate three-dimensional end-member morphology in lateral view for each principal component. Numbered nodes on the wireframe models correspond to the measured landmarks illustrated in Figure 4. Individuals with the same crural morph are denoted with ellipses. Ellipses have no statistical meaning. A complete list of PC scores is available from the authors for all analyses.

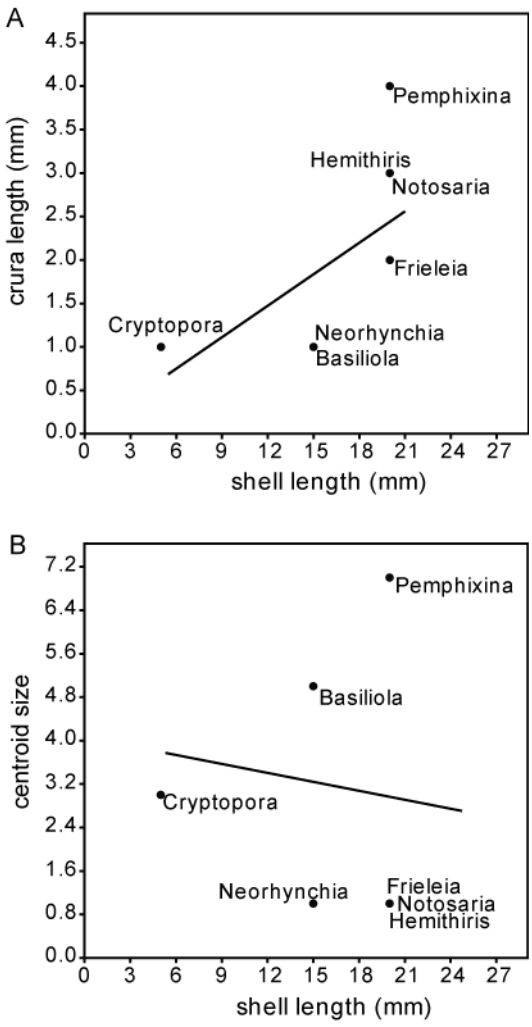

Figure 6. A, Crura length versus shell length in juvenile and adult Recent rhynchonellides. Crura and shell length are averages estimated from at least two photographs per species in literature sources (Savage et al., 2002; Manceñido et al. 2007). Crura length is measured from base of crus to tip of crus. Shell length is the length of the ventral valve. Crura length and shell length are not significantly correlated (r = 0.70, p = 0.07). B, Centroid size versus shell length in juvenile and adult Recent rhynchonellides. Centroid size is the average centroid size of each species (the centroid size of each individual was previously calculated in this analysis). Centroid size and shell length are not significantly correlated (r = -0.09, p = 0.85) among all species.

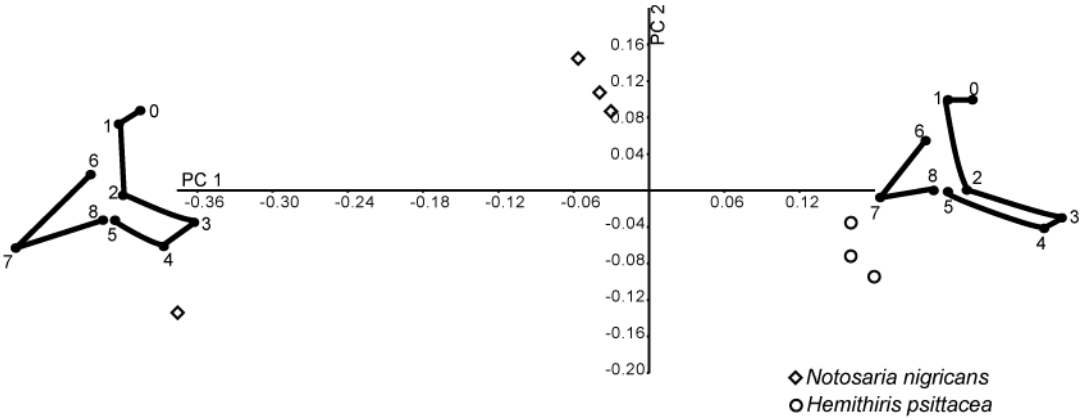

Figure 7. PCA of raduliform crura of adult *Notosaria nigricans* and *Hemithiris psittacea.* Size has been standardized. *Notosaria* and *Hemithiris* form two distinct clusters within the raduliform ellipse in Figure 4. Raduliform crura exhibit interspecific variability, as illustrated in this PCA. However, the one *Notosaria* outlier greatly affects the distribution of the remaining specimens. The outlier is much shorter and wider than the other specimens of *Notosaria*, indicating intraspecific variability of the crura. Variation along PC1 is associated with crural length, width, and divergence. PC 1 accounts for 64.93% of the total variance in data. The raduliform crura of *Hemithiris* tend to be more elongate, while the raduliform crura of *Notosaria* are shorter and wider. Wireframe models illustrate end-member morphology in lateral view for PC 1. Numbered nodes on the wireframe models correspond to the measured landmarks illustrated in Figure 4.

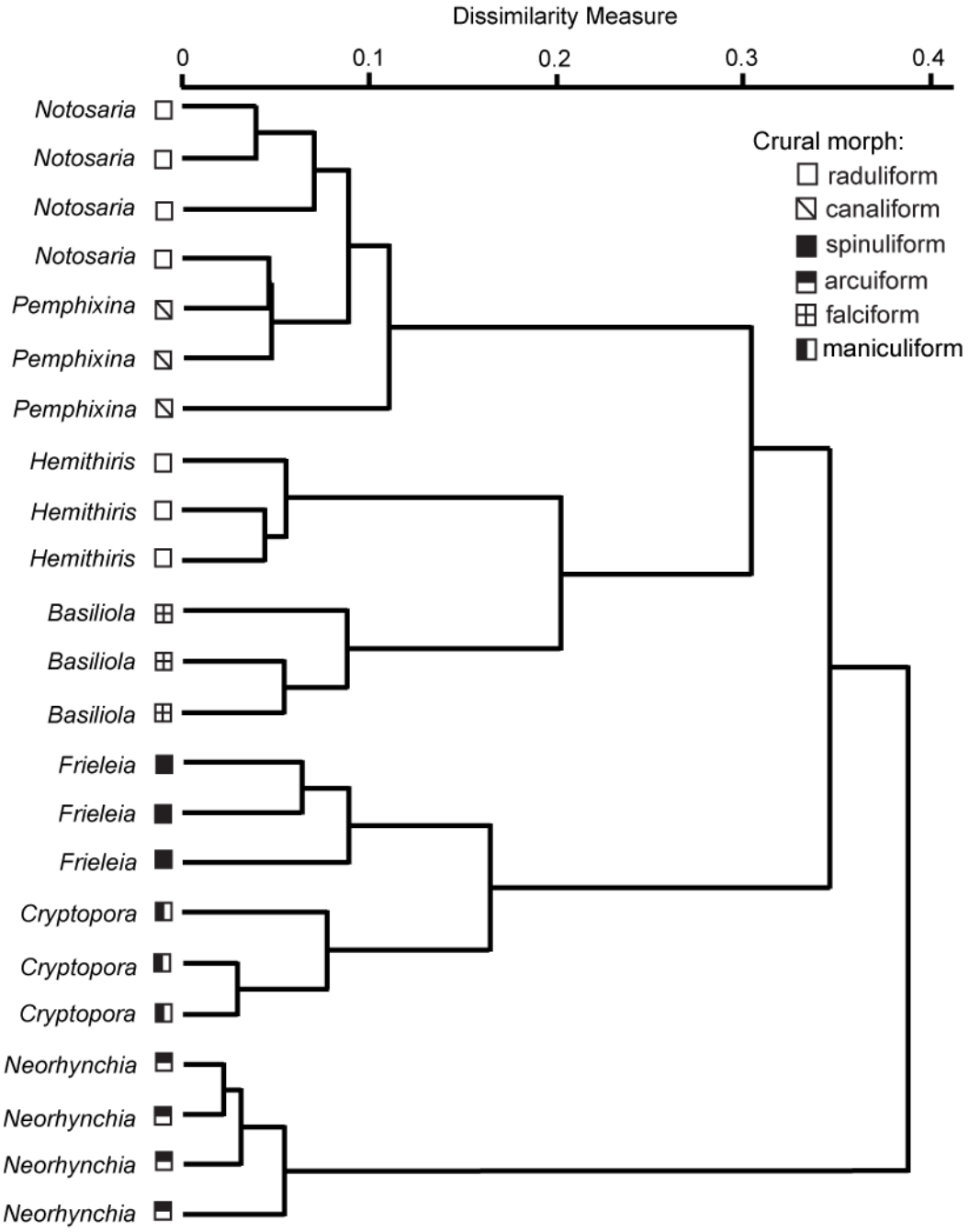

Figure 8. Single linkage cluster analysis of adult crura. Cluster analysis was performed using the scores on the first three principal components together. The dissimilarity measure is a measure of the Euclidean distances between specimens. Euclidean distance is a measure of the straight line distance between two points in space. Crural types tend to cluster together, with the exception of the raduliform and canaliform types. The specimens of each genus also cluster together with the exception of *Notosaria*. The one *Notosaria* individual that clusters with *Pemphixina* is the outlier in Figure 7. This *Notosaria* individual is shorter and wider than the remaining *Notosaria*.